Journal of Materials Chemistry A

PAPER

View Article Online
View Journal | View Issue

Cite this: J. Mater. Chem. A, 2014, 2, 9751

Mesoporous carbon/silicon composite anodes with enhanced performance for lithium-ion batteries

Yunhua Xu, Yujie Zhu and Chunsheng Wang*

Received 8th April 2014
Accepted 29th April 2014

DOI: 10.1039/c4ta01691b

www.rsc.org/MaterialsA

Silicon offers the highest theoretical capacity among all anode materials investigated for Li-ion batteries, making it a promising alternative anode to the currently used graphite. However, Si anodes still face significant challenges for commercialization because of the poor cycling performance induced by the huge volume change (300%) that occurs during the insertion/extraction of lithium ions. In this paper, we report a mesoporous C/Si composite synthesized by an organic–organic self-assembly of a triblock copolymer and a resorcinol–formaldehyde resin. Large number of hydroxyl groups of the RF resin directs the formation of a mesostructure and coating/dispersion of the Si nanoparticles by strong hydrogen bonding interactions. The mesoporous carbon matrix efficiently accommodates the volume change of nano-Si and maintains the integrity of the nano-Si electrodes. Significant improvement in the electrochemical performance was demonstrated in comparison with the bare Si nanoparticle anodes. In addition, the synthesis method can be easily scaled up for mass production.

1. Introduction

Lithium-ion batteries, the dominating power sources for portable electronic devices, have been recognized as the most promising technology for next generation energy storage for electric vehicles and renewable energy. However, graphite anodes used in the current commercial Li-ion batteries have a limited capacity (372 mA h g^{-1}), which restricts their application for electric vehicles. As one of the most promising alternative anodes to graphite, silicon offers a theoretical capacity of 3579 mA h g^{-1} upon full intercalation state of $Si_{15}Li_4$ at room temperature, which is ten times higher than that of graphite; till date, this is the highest capacity among all the anode materials investigated.

However, Si anodes suffer from a huge volume change (300%) that occurs during the insertion/extraction of lithium ions, resulting in particle pulverization, losing electric connection between the Si particles and the current collector and the continuous growth of solid–electrolyte interface (SEI) film, and thus fast capacity fading.[1,2] In addition, the low electronic conductivity of Si also lowers the power density. Extensive efforts have been made to improve the cycling stability and power density.[3–25] The most successful strategies have used graphene,[6–9] carbon tubes,[10–15] hollow or porous carbon[16–23] to accommodate the Si stress/strain induced by volume change and enhance the electronic conductivity. However, most C/Si composite materials are synthesized using complicated and expensive high-temperature chemical vapor deposition[6,10–12,14,15,22] or hard template[13,16–18,20] methods, which limits practical applications for mass-production.

Mesoporous carbon, possessing good conductivity, high resiliency, good mechanical strength and large porosity, is an ideal support matrix for Si nano-particles, which can efficiently alleviate the stress/strain and volume change of Si particles. Among all the reported synthesis methods for mesoporous carbon, the most facile and cost-efficient route is the organic–organic self-assembly method using commercial precursor materials followed by a carbonization process,[26–29] in which phenolic resins and triblock copolymers of poly(ethylene oxide)-*b*-poly(propylene oxide)-*b*-poly(ethylene oxide) (PEO-PPO-PEO) are used as carbon precursor and structure-directing agents, respectively. Hydrogen bonding between the hydroxyl groups of phenolic resin and the polyethylene (PEO) chains of copolymers direct the formation of mesostructures. Recently, Park *et al.* reported the synthesis of a mesoporous carbon/Si nanoparticle composite using triblock copolymer of Pluronic F127 and phenol–formaldehyde (F) polymer as the template agent and carbon precursor, respectively.[30] Si nanoparticles were well coated with carbon and uniformly distributed in the mesoporous carbon due to hydrogen bonding interactions between a large number of hydroxyl groups (–OH) in the phenol–formaldehyde resin and an oxide layer on the surface of the Si nanoparticles.

It has been shown that the density of the hydroxyl groups in the phenolic resin is a key factor for the formation of mesostructures and the surface coating of Si particles.[27,28,31] Resorcinol (R) has double the number of hydroxyl groups than phenol, offering a greater driving force for self-assembly and

Department of Chemical and Biomolecular Engineering, University of Maryland, College Park, MD 20742, USA. E-mail: cswang@umd.edu; Fax: +1 301 405 0523; Tel: +1 301 405 0352

interaction with the Si/resin. In fact, fine encapsulation/coating of Si nanoparticles with RF-resin carbon has been reported and an improved capacity and cycling stability for the RF-based C/Si composites was obtained.[32–35]

Recently, we have successfully fabricated a sponge-like mesoporous C/Sn composite using the RF resin as carbon precursor and the triblock copolymer of poly(ethylene oxide)-*b*-poly(propylene oxide)-*b*-poly(ethylene oxide) (EO106-PO70-EO106, Pluronic F127) as the template agent, where SnO_2 nanoparticles were dispersed in the RF resin/F127 precursor matrix followed by carbonization.[36] In the mesoporous C/Sn composite, the mesoporous carbon matrix can efficiently accommodate the volume change of Sn nanoparticles, thus enhancing the cycling stability. In this study, this strategy was used for Si anodes. The large number of hydroxyl groups on the surface of Si and the RF resin gives rise to strong interactions between them *via* hydrogen bonding, which ensures a fine coating and dispersion of Si nanoparticles within the mesoporous carbon matrix. Significant improvement in electrochemical performance was also demonstrated.

2. Experimental

2.1 Synthesis of mesoporous C/Si nanoparticle composite

The synthesis of mesoporous C/Si composite materials consisted of three steps: preparation of precursor solution and dispersion of Si nanoparticle, *in situ* polymerization, and carbonization. All materials were purchased from Sigma-Aldrich and were used without further purification. 0.3 g Si nanoparticles (<100 nm) were dispersed in 20 mL *N*,*N*-dimethylformamide (DMF) through ultrasonication. Meanwhile, the precursor solution was prepared by dissolving 0.165 g resorcinol (R), 0.1 g triblock copolymer Pluronic F127 and 0.03 g 37% HCl aqueous solution in 5 mL DMF, where the triblock copolymer and HCl functioned as the soft-template and catalyst, respectively. When the solution turned clear, 0.195 g 37% formaldehyde (F) aqueous solution was added. After 30 min of vigorous stirring, the solution was stirred for another 30 min at 80 °C to prepolymerize the precursors of resorcinol and formaldehyde. Then, the resulting solution was added into the Si dispersion and subjected to ultrasonic treatment. The mixture was dried while stirring overnight at 100 °C and further cured in an oven at 100 °C for 24 h. Finally, the polymer/nano-Si composite was carbonized at 400 °C for 3 h and then 700 °C for an additional 3 h in flowing argon with heating ramp of 2 °C min^{-1}. Pure mesoporous carbon without Si was also synthesized using the same procedure described above.

2.2 Material characterizations

Scanning electron microscopy (SEM) and transmission electron microscopy (TEM) images were taken on a Hitachi SU-70 analytical ultra-high resolution SEM (Japan) and JEOL (Japan) 2100F field emission TEM, respectively. Thermogravimetric analysis (TGA) was carried out using thermogravimetric analyzer (TA Instruments, USA) with a heating rate of 10 °C min^{-1} in air. BET specific surface area and pore size and volume were analyzed using N_2 absorption on TriStar 3020 (Micromeritics Instrument Corp., USA).

2.3 Electrochemical Measurements

The mesoporous C/Si composite was mixed with carbon black and sodium carboxymethyl cellulose (CMC) binder to form a slurry at a weight ratio of 70 : 15 : 15. The mesoporous C/Si electrode with active material loading of ~1 mg cm^{-2} was prepared by casting the slurry onto a copper foil using a doctor blade and dried overnight in a vacuum oven at 100 °C. Coin cells were assembled with lithium foil as a counter electrode, 1 M $LiPF_6$ in a mixture of fluoroethylene carbonate–dimethyl carbonate (FEC–DMC, 1 : 1 by volume) as the electrolyte and Celgard®3501 (Celgard, LLC Corp., USA) as the separator. Cells with bare nano-Si electrodes were also fabricated using the same procedure. Electrochemical performance was tested using Arbin battery test station (BT2000, Arbin Instruments, USA) at a voltage range of 0.02–1.5 V. Capacity was calculated on the basis of Si mass. Impedance data were recorded using Solatron 1260/1287 Electrochemical Interface (Solartron Metrology, UK).

3. Results and discussion

The mesoporous carbon was synthesized using a resorcinol–formaldehyde (RF) polymer as the carbon source and a triblock copolymer of Pluronic F127 as the sacrificial template to form pores.[26–29] Fig. 1 illustrates the formation of the self-assembly nanostructure of RF-resin/F128 and the coating process of Si nanoparticles. The RF resins contains a large number of hydroxyl groups, which allow them to form hydrogen bonds with the hydrophilic blocks of the triblock copolymer F127 or the hydroxyl groups on the surface of the Si nanoparticles. Thus, a thin layer of RF resin was coated on the surface of the Si nanoparticles. Meanwhile, the copolymer surfactant of Pluronic F127 and RF resin also forms mesophase structure matrix under the self-assembly process. It should be noted that different surface energy of the Si surface and the RF resin may affect the self-assembly behavior, especially in the area close to the surface of the Si nanoparticles.[37] The triblock copolymer decomposed in the subsequent carbonization steps to create pores, and the RF polymer framework was carbonized to form the carbon walls or coating carbon for the Si nanoparticles.

Fig. 2a–d shows the SEM images of the pure mesoporous carbon and the mesoporous carbon/Si composite. A well-defined and uniform pore structure with a pore size of ~10 nm and ~5 nm carbon walls was observed in the mesoporous carbon (MC) (Fig. 2a). In contrast to the uniform pores and highly ordered structure of the pure carbon, the mesoporous structure was clearly observed in the C/Si composite but with a random geometric pore shape and order (Fig. 2c and d). This is believed to be associated with the difference in surface energy between the Si nanoparticles and the RF resin. In Fig. 2c, the peeling-off of the Si particles (marked with red circles) show as bright cycles on the edge and a lower clarity than the surrounding area. The high resolution TEM image (Fig. 2f) further reveals that a thin layer of carbon with a thickness of

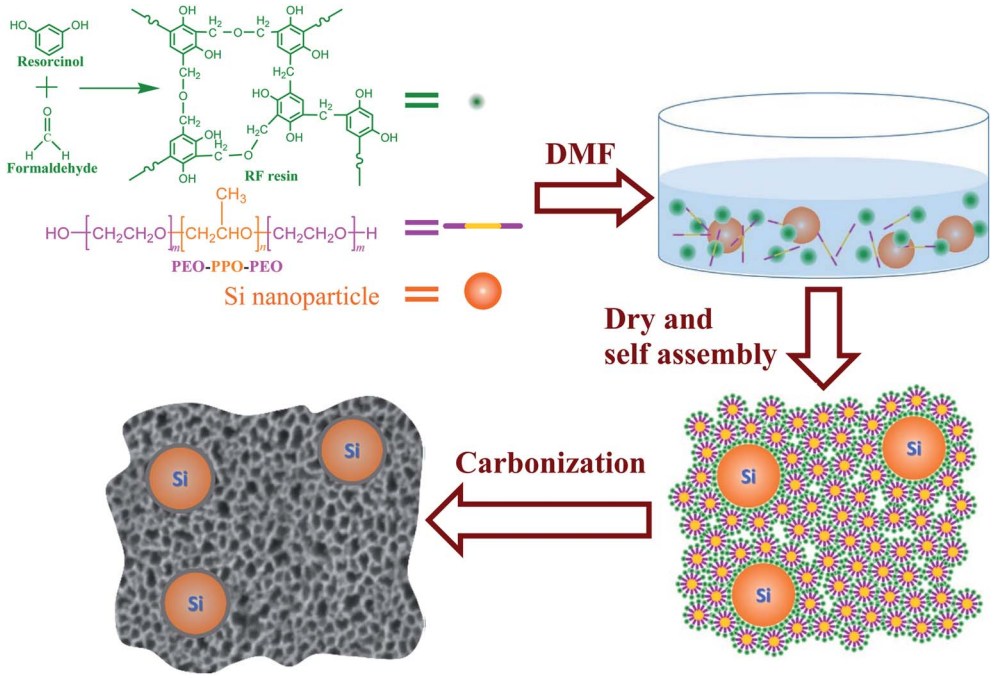

Fig. 1 Schematic illustration of the synthesis of the mesoporous C/Si composite.

~5 nm is uniformly coated on the surface of Si nanoparticles, as marked with red dashed lines in Fig. 2f, which strongly revealed that a thin layer of carbon was coated onto the surface of the Si nanoparticles. These findings confirm the strong interaction between the RF resin and Si surface. The low-magnification SEM (Fig. 2b) and low-resolution TEM images (Fig. 2e) of the porous C/Si composite show a uniform distribution of Si nanoparticles in the carbon matrix.

Very thin carbon walls form a continuous carbon network to provide an efficient electron transportation pathway, while the continuous pores function as ion transport channels and strain absorbers. As a combination of the resiliency of carbon walls and the large number of mesopores between the carbon walls in the carbon matrix, the mesoporous carbon matrix provides a flexible mechanical support for the nano-Si during lithiation/delithiation.

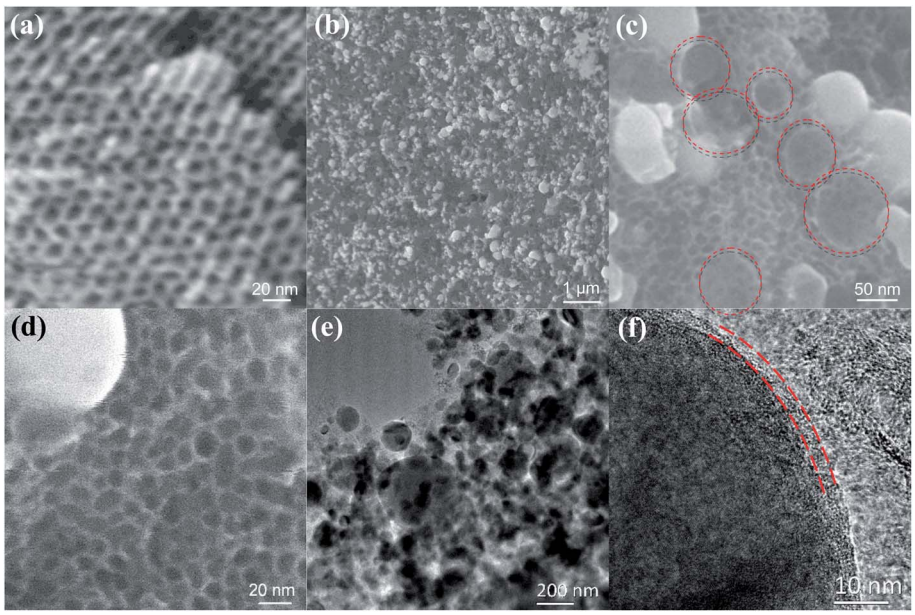

Fig. 2 SEM images of (a) the pure mesoporous carbon and (b–d) the mesoporous C/Si composites. (e and f) TEM images of the mesoporous C/Si composites.

The mesoporous structure in the mesoporous C/Si composite was further characterized by N_2 adsorption measurement. Fig. 3a depicts the adsorption isotherm. The Brunauer–Emmett–Teller (BET) specific surface area and pore volume of the MC/Si composite are 210 m^2 g^{-1} and 0.29 cm^3 g^{-1}, respectively. The large pore volume of the carbon matrix could alleviate stain/stress induced by the large volume change of nano-Si, and the large specific surface area improves the electrochemical reaction kinetics. The pore size distribution from Barrett–Joyner–Halenda (BJH) measurement shows that the average pore size is 9.8 nm (Fig. 3b), which is in good agreement with that observed by the SEM and TEM images in Fig. 2.

The carbon content in the mesoporous C/Si composite was determined using thermogravimetric analysis (TGA) in air. Fig. 4 shows the thermogravimetric curve of the mesoporous C/Si composite. No weight loss was observed below 450 °C, indicating that the mesoporous C/Si composite is thermally stable in ambient air. A sharp mass loss occurred between 450 and 580 °C due to carbon decomposition. A slight increase in the high temperature range was attributed to Si oxidation. The Si content in the composite was calculated to be 76% by weight.

The electrochemical performance of the mesoporous C/Si composite was investigated using coin cells. Fig. 5a shows the charge/discharge profiles of the mesoporous C/Si composite during the initial 5 cycles. In the first lithiation, the potential gradually decreases with Li content and is followed by a long flat discharge plateau at ~0.08 V. The slope potential decrease at the MC/Si anodes in the high potential area (Fig. 5a) is mainly attributed to the lithiation of the mesoporous carbon (Fig. 4b), while the flat discharge plateau at ~0.08 V is a typical lithiation behavior of crystal Si anodes.[3–5] The small plateaus at 0.8 V in the first discharge of C/Si anodes (Fig. 5a) that disappeared in the following cycles are attributed to the formation of SEI films due to the decomposition of the electrolytes on porous C, as shown in Fig. 5b. The formation of SEI films lead to irreversible capacity, consuming Li ions that are a limited resource usually stored and carried by the cathode upon cell assembly, thus lowering the coulombic efficiency. The mesoporous C/Si composites deliver charge capacities of 1461 mAh g^{-1} with a coulombic efficiency of 54%. The high irreversible capacity in the first cycle is mainly due to the large surface area of the mesoporous C/Si composite, and a large amount of SEI film was formed on the surface of the mesoporous carbon (Fig. 5b). This is confirmed by the ultralow coulombic efficiency of 34% for the pure mesoporous carbon anodes (Fig. 5c). After two cycles, the coulombic efficiency of the mesoporous C/Si composite jumped to higher than 97%, indicating a good reversibility of the mesoporous C/Si composite. The charge process shows a slope plateau between 0.2 and 0.7 V, which is a typical feature of the delithation reaction of amorphous Li_xSi. In the following cycles, the typical electrochemical behavior of amorphous Si anodes were observed with discharge/charge slopes at 0.2/0.5 V, respectively. The phase transition from crystalline to amorphous after the first cycle is a typical behavior of Si anodes.[3–5]

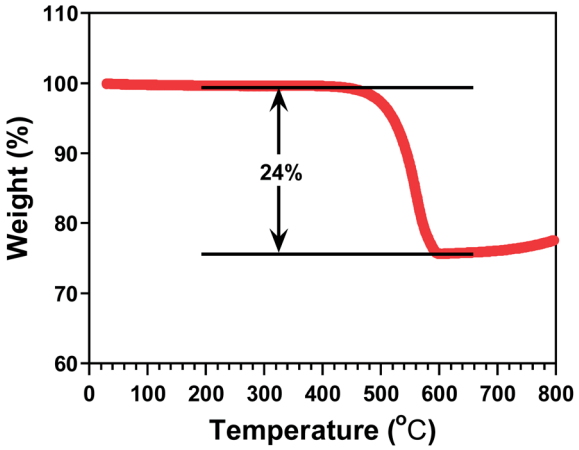

Fig. 4 Thermogravimetric analysis (TGA) curve of the mesoporous C/Si composites in air.

To examine the stability of the mesoporous C/Si composite, mesoporous C/Si anodes were cycled between 0.02–1.5 V at a current density of 500 mA g^{-1}. For comparison, the electrochemical performance of the bare nano-Si and mesoporous carbon were also tested under the same conditions. Fig. 5c shows the cycling stabilities of mesoporous carbon, bare nano-Si and the mesoporous C/Si composites. Compared with the bare Si nanoparticles, the cycling performance of the mesoporous C/Si composite is significantly improved. The mesoporous C/Si composite delivered a reversible capacity of 1410 mA h g^{-1} in the first cycle and retained a capacity of 1018 mA h g^{-1} after 100 charge/discharge cycles, which is three

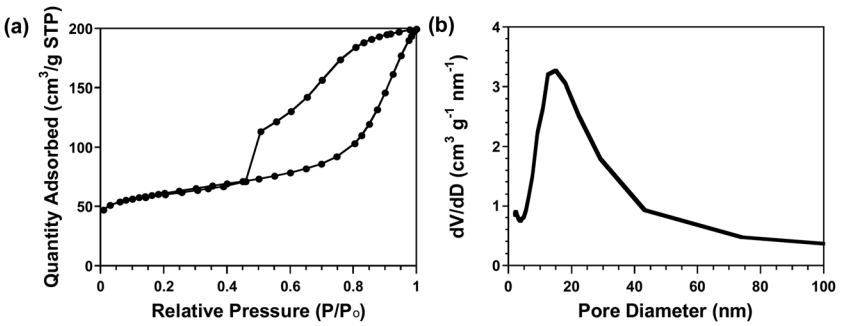

Fig. 3 (a) N_2 adsorption/desorption isotherm and (b) pore size distribution of the mesoporous C/Si composites.

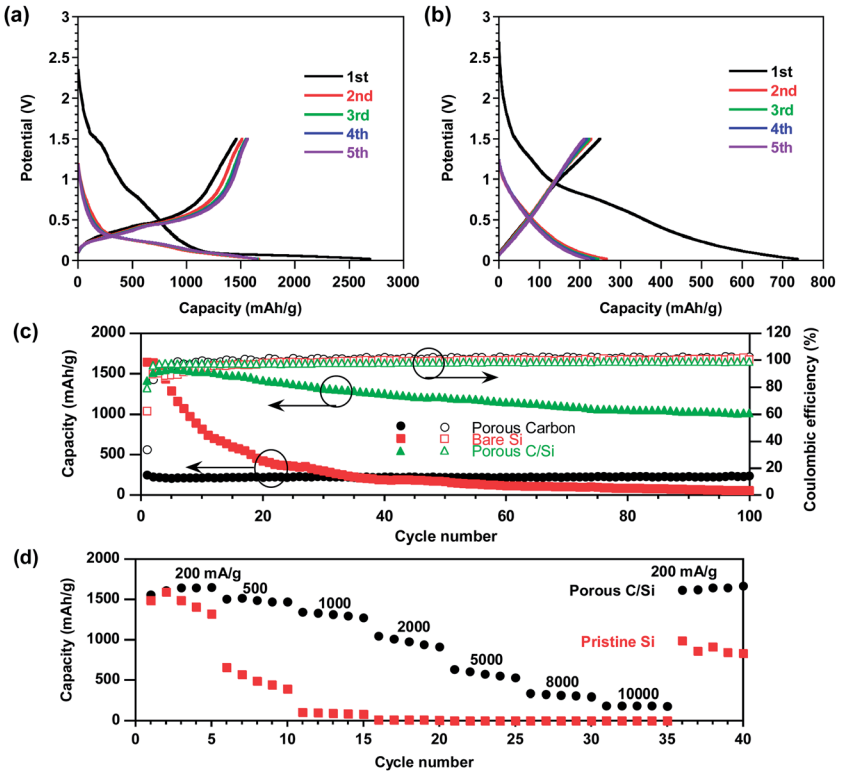

Fig. 5 Charge/discharge profiles in the first five cycles of (a) the mesoporous C/Si composites and (b) pure mesoporous carbon. (c) Cycling performance and (d) rate capability of the mesoporous C/Si composite, bare Si and mesoporous carbon anodes.

times higher than graphite. The cycling performance of the porous C/Si composite is much better than that of the previous porous C/Si composites synthesized using phenolic resol precursor (700 mA h g^{-1} after 50 cycles)[30] and nano $CaCO_3$ template (594 mA h g^{-1} after 50 cycles).[38] In contrast, although bare Si nanoparticles show a little higher reversible capacity of 1644 mA h g^{-1} in the first cycle, only 59 mA h g^{-1} retained after 100 cycles, which revealed a fast capacity fading. Mesoporous carbon shows a high cycling stability but the capacity of 220 mA h g^{-1} is too low. The role of pure mesoporous carbon is to provide an electrochemically stable mechanical support. The capacity and stability of the RF porous C/Si anodes are superior to those of the RF coated Si anodes[32–35] and phenol–formaldehyde-based porous C/Si anodes.[30] The enhancement in cycling performance is undoubtedly attributed to the incorporation of the mesoporous carbon matrix made of the RF resin.

The rate performance of the mesoporous C/Si composite and bare nano-Si anodes is compared in Fig. 5d. In addition to the poor cycling stability, the bare nano-Si anodes also suffer fast capacity roll-off as the current increased, and fail to deliver any capacity when the current was increased to 1000 mA g^{-1}. On the contrary, a capacity of ~1220 mA h g^{-1} was retained at 1000 mA g^{-1} for the mesoporous C/Si composite. Even at a very high current of 10 A g^{-1}, a capacity retention of ~180 mA h g^{-1} was achieved for the mesoporous C/Si anodes. The improved rate capability of the mesoporous C/Si composite is attributed to the large surface area of the mesoporous structure and conductive carbon network.

The electrochemical reaction kinetics of the mesoporous C/Si composite and bare nano-Si anodes was compared using electrochemical impedance spectroscopy (EIS) with a voltage amplitude of 10 mV in the frequency range of 10 MHz to 0.01 Hz. Fig. 6 shows the Nyquist plots of the fresh mesoporous C/Si and bare Si anodes. The impedance spectra consists of a depressed semicircle at high frequencies and a slopping line at low frequencies. The depressed semicircle at high frequencies is associated with two overlapped interface impedances (*i.e.* SEI and charge transfer), and the low-frequency line corresponds to

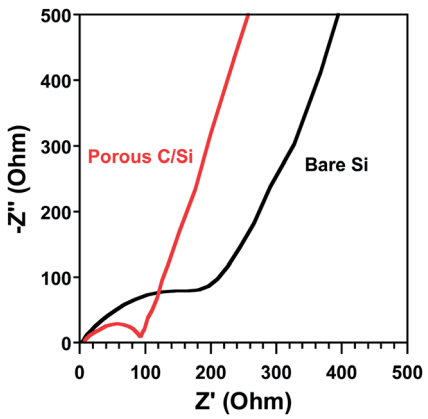

Fig. 6 Nyquist plot of the fresh mesoporous C/Si composite and bare Si anodes.

lithium ion diffusion. It was clear that the mesoporous C/Si composite experienced much lower interface impedance compared with bare nano-Si anodes, indicating a lower reaction resistance for the mesoporous C/Si composite, and thus a better rate capability.

The enhancement in cycling stability and rate capability of the mesoporous C/Si composite is attributed to the merits of the mesoporous carbon matrix, including: (1) the large pore volume offers void space to accommodate the volume change; (2) the thin resilient carbon walls and coating layer on Si surface provide a mechanical support to enable good electric contact between Si nanoparticles and carbon matrix; and (3) the large specific surface area and continuous pore channels ensure a fast charge transfer and ion transport.

4. Conclusions

A mesoporous C/Si composite was successfully synthesized by *in situ* polymerization and carbonization. Si nanoparticles were uniformly dispersed in the well-defined mesoporous carbon matrix, which offers void space and mechanical support to accommodate large volume changes and the stress induced by nano-Si. In comparison with the bare Si nanoparticles and other C-coated Si anodes, a significantly improved electrochemical performance was obtained for the mesoporous C/Si composite anodes. After 100 charge/discharge cycles, the mesoporous C/Si composite anodes retained a capacity of 1018 mA h g^{-1}, which is much higher than that of bare nano-Si anodes (59 mA h g^{-1}). A better rate capability was also demonstrated for the mesoporous C/Si composite anodes. In addition, the synthesis method is facile and simple and can be easily scaled up, making it attractive for mass manufacture for large-scale applications.

Acknowledgements

The authors gratefully acknowledge the support of the Army Research Office under Contract W911NF1110231.

References

1 U. Kasavajjula, C. S. Wang and A. J. Appleby, *J. Power Sources*, 2007, **163**, 1003.
2 H. Wu and Y. Cui, *Nano Today*, 2012, **7**, 414.
3 C. Chan, H. Peng, G. Liu, K. Mcilwrath, X. F. Zhang, R. A. Huggins and Y. Cui, *Nat. Nanotechnol.*, 2008, **3**, 31.
4 H. Wu, G. Chan, J. W. Choi, I. Ryu, Y. Yao, M. T. McDowell, S. W. Lee, A. Jackson, Y. Yang, L. Hu and Y. Cui, *Nat. Nanotechnol.*, 2012, **7**, 310.
5 I. Kovalenko, B. Zdyrko, A. Magasinski, B. Hertzberg, Z. Milicev, R. Burtovyy, I. Luzinov and G. Yushin, *Science*, 2011, **334**, 75.
6 K. Evanoff, A. Magasinski, J. Yang and G. Yushin, *Adv. Energy Mater.*, 2011, **1**, 495.
7 Y. Wen, Y. J. Zhu, A. Langrock, A. Manivannan, S. H. Ehrman and C. S. Wang, *Small*, 2013, **9**, 2810.
8 X. Zhou, Y.-X. Yin, L.-J. Wan and Y.-G. Guo, *Adv. Energy Mater.*, 2012, **2**, 1086.
9 J. Ji, H. Ji, L. L. Zhang, X. Zhao, X. Bai, X. Fan, F. Zhang and R. S. Ruoff, *Adv. Mater.*, 2013, **25**, 4673.
10 A. Gohier, B. Laïk, K.-H. Kim, J.-L. Maurice, J.-P. Pereira-Ramos, C. S. Cojocaru and P. T. Van, *Adv. Mater.*, 2012, **24**, 2592.
11 W. Wang and P. N. Kumta, *ACS Nano*, 2010, **4**, 2233.
12 L. Hu, H. Wu, Y. Gao, A. Cao, H. Li, J. Mcdough, X. Xie, M. Zhou and Y. Cui, *Adv. Energy Mater.*, 2011, **1**, 523.
13 M.-H. Park, M. G. Kim, J. Joo, K. Kim, J. Kim, S. Ahn, Y. Cui and J. Cho, *Nano Lett.*, 2009, **9**, 3844.
14 B. Hertzberg, A. Alexeev and G. Yushin, *J. Am. Chem. Soc.*, 2010, **132**, 8548.
15 B. Wang, X. Li, X. Zhang, B. Luo, Y. Zhang and L. Zhi, *Adv. Mater.*, 2013, **25**, 3560.
16 N. Liu, H. Wu, M. T. McDowell, Y. Yao, C. Wang and Y. Cui, *Nano Lett.*, 2012, **12**, 3315.
17 H. Wu, G. Zheng, N. Liu, T. J. Carney, Y. Yang and Y. Cui, *Nano Lett.*, 2012, **12**, 904.
18 D. S. Jung, T. H. Hwang, S. B. Park and J. W. Choi, *Nano Lett.*, 2013, **13**, 2092.
19 Y.-S. Hu, P. Adelhelm, B. M. Smarsly and J. Maier, *ChemSusChem*, 2010, **3**, 231.
20 H. Kim, B. Han, J. Choo and J. Cho, *Angew. Chem., Int. Ed.*, 2008, **47**, 10151.
21 R. Yi, F. Dai, M. L. Gordin, S. Chen and D. Wang, *Adv. Energy Mater.*, 2013, **3**, 295.
22 A. Magasinski, P. Dixon, B. Hertzberg, A. Kvit, J. Ayala and G. Yushin, *Nat. Mater.*, 2010, **9**, 353.
23 T. H. Hwang, Y. M. Lee, B.-S. Kong, J.-S. Seo and J. W. Choi, *Nano Lett.*, 2012, **12**, 802.
24 S. H. Ng, J. Wang, D. Wexler, K. Konstantinov, Z.-P. Guo and H.-K. Liu, *Angew. Chem., Int. Ed.*, 2006, **45**, 6896.
25 J. Deng, H. Ji, C. Yan, J. Zhang, W. Si, S. Baunack, S. Oswald, Y. Mei and O. G. Schmidt, *Angew. Chem., Int. Ed.*, 2013, **52**, 2326.
26 Y. Meng, D. Gu, F. Zhang, Y. Shi, H. Yang, Z. Li, C. Yu, B. Tu and D. Y. Zhao, *Angew. Chem., Int. Ed.*, 2005, **44**, 7053.
27 Y. Meng, D. Gu, F. Zhang, Y. Shi, L. Cheng, D. Feng, Z. Wu, Z. Chen, Y. Wan, A. Stein and D. Y. Zhao, *Chem. Mater.*, 2006, **18**, 4447.
28 C. Liang and S. Dai, *J. Am. Chem. Soc.*, 2006, **128**, 5316.
29 S. Tanaka, N. Nishiyama, Y. Egashira and K. Ueyama, *Chem. Commun.*, 2005, 2125.
30 J. Park, G.-P. Kim, I. Nam, S. Park and J. Yi, *Nanotechnology*, 2013, **24**, 025602.
31 D. Zhao, Q. Huo, J. Feng, B. F. Chmelka and G. D. Stucky, *J. Am. Chem. Soc.*, 1998, **120**, 6024.
32 J.-K. Lee, M. C. Kung, L. Trahey, M. N. Missaghi and H. H. Kung, *Chem. Mater.*, 2009, **21**, 6.
33 G. X. Wang, J. H. Ahn, J. Yao, S. Bewlay and H. K. Liu, *Electrochem. Commun.*, 2004, **6**, 689.
34 Y. S. Jung, K. T. Lee and S. M. Oh, *Electrochim. Acta*, 2007, **52**, 7061.
35 T. Hasegawa, S. R. Mukai, Y. Shirato and H. Tamon, *Carbon*, 2004, **42**, 2573.

36 Y. H. Xu, J. C. Guo and C. S. Wang, *J. Mater. Chem.*, 2012, **22**, 9562.
37 K. Wang, W. Zhang, R. Phelan, M. A. Morris and J. D. Holmes, *J. Am. Chem. Soc.*, 2007, **129**, 13388.
38 X. Shen, D. Mu, S. Chen, B. Xu, B. Wu and F. Wu, Si/mesoporous carbon composite as an anode material for lithium ion batteries, *J. Alloys Compd.*, 2013, **552**, 60.